Flexure Mechanisms with Variable Stiffness and Damping Using Layer Jamming

Buse Aktaş[1] and Robert D. Howe[1]

Abstract— **Flexures provide precise motion control without friction or wear. Variable impedance mechanisms enable adaptable and robust interactions with the environment. This paper combines the advantages of both approaches through layer jamming. Thin sheets of complaint material are encased in an airtight envelope, and when connected to a vacuum, the bending stiffness and damping increase dramatically. Using layer jamming structures as flexure elements leads to mechanical systems that can actively vary stiffness and damping. This results in flexure mechanisms with the versatility to transition between degrees of freedom and degrees of constraint and to tune impact response. This approach is used to create a 2-DOF, jamming-based, tunable impedance robotic wrist that enables passive hybrid force/position control for contact tasks. Keywords: Compliant Joint/Mechanism, Compliance and Impedance Control, Mechanism Design**

I. INTRODUCTION

Flexures use elastic structures that deform in bending to allow motion in desired directions (degrees of freedom) while constraining motion in others (degrees of constraint). Compared to other bearing systems, they are simple and inexpensive to manufacture, have no friction or stiction, and do not require maintenance or lubrication [1], [2]. These advantages have made flexures popular as motion control elements for robotics (e.g. [3]–[6]).

There is growing interest in providing tunable impedance capabilities in robots to enable adaptable and robust interaction with their environments. This has been achieved with a variety of methods from feedback control algorithms to variable impedance actuators and mechanisms. [7]–[9] Variable stiffness and damping structures have been used

to generate passive compliance in order to tune the impact response of robots as well as for hybrid force/position control during complex interactive tasks. [9]–[13]

Unfortunately coupling existing variable impedance mechanisms to flexure systems is not trivial. Most variable stiffness and damping actuators are designed for purely rotational or translational motion. In contrast, simple single-beam flexures do not have a fixed center of rotation, and compound flexures rarely follow a strictly linear path during motion. This poses a challenge in combining the advantages of flexure systems with variable impedance mechanisms.

This study addresses this challenge by creating flexure mechanisms with inherent variable impedance, using layer jamming. In layer jamming, a pressure gradient is applied to a stack of compliant layers, increasing the bending stiffness of the structure by inducing frictional and kinematic coupling between the layers. Layer jamming elements provide a significantly larger range in stiffness variation than most variable stiffness mechanisms, and like flexures, they are low cost, low profile and easy to fabricate. They have been used in a variety of robotic applications to achieve dexterous and adaptable behavior. [14]–[16]

This paper begins by introducing jamming-based flexure mechanisms, which provide flexures the adaptability to switch between low and high stiffness, allowing transition between a degree of freedom and a degree of constraint. It also enables variable damping, which is used to tune impact response. We characterize the mechanical behavior of these mechanisms with a model, capturing the effects of the design parameters. We then propose a 2-DOF jamming-based tunable impedance robotic wrist with flexure mechanisms, and experimentally demonstrate its performance in manipulation tasks.
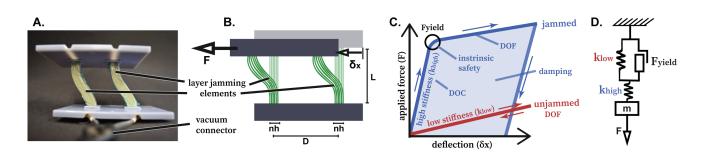

Fig. 1. Jamming-based flexure mechanism. **A.** Physical prototype. **B.** Diagram showing relevant parameters. **C.** Force-deflection plot characterizing mechanical behavior under jammed and unjammed conditions, showing Degrees of Freedom (D.O.F.) where low stiffness allows motion and Degrees of Constraint (D.O.C.) where high stiffness limits motion. **D.** Lumped parameter model of layer jamming structure that captures static and dynamic behavior.

II. Flexures With Layer Jamming

Using layer jamming bending elements in flexures can produce mechanisms that combine the advantages of both. Layer jamming structures can be formed by placing a stack of paper inside an airtight plastic envelope. When this plastic bag is connected to a vacuum source, the external air pressure forces the layers together. The resulting friction couples the layers into a coherent beam with a far greater bending stiffness than when the individual layers are not compressed. For full details of the mechanical behavior of layer jamming structures, please see [16].

We begin the analysis of the behavior of jamming-based flexures with a simple parallel flexure mechanism made of two parallel leaf-spring layer jamming bending elements (Fig. 1A,B). Each bending element is connected rigidly at both ends, holding the ends at a constant angle (i.e. a double cantilever configuration). Treating the lower mounting as fixed, as forces are applied to the upper mounting the mechanism articulates side-to-side following a curved trajectory, while the mounting elements remain parallel.

A. Modeling jamming-based flexures

With boundary conditions of constant angles at ends, and using Euler-Bernoulli beam theory, the stiffness of the parallel flexure along direction of motion is determined from the geometry and material properties of the elements [1], [2]

$$k_{\delta_x F_x} = \frac{24EI}{L^3} \tag{1}$$

where E is the Young's modulus, I is the bending moment of inertia, and L is the flexure length. This stiffness is constant in traditional non-tunable flexures. With layer jamming elements instead of continuous beams, stiffness is varied by altering the moment of inertia I. When unjammed, the layers act effectively independently sliding freely with respect to each other, so the effective moment of inertia is simply the sum of the individual layer values. But when jammed, the layers form a cohesive beam with thickness equal to the sum of the layers' thicknesses. Given the width b, thickness h and number of the constituent layers n in each jamming element, I can be determined for the two states [16]

$$I_{unjammed} = \frac{nbh^3}{12} \tag{2}$$

$$I_{jammed} = \frac{n^3bh^3}{12} \tag{3}$$

This introduces the ability to drastically change the stiffness on command, allowing alternation between a degree of freedom and a degree of constraint. When the flexure elements are jammed, the structure is stiff and resists motion (blue curve in Fig. 1C); when unjammed, the flexure is compliant (red curve). The full stiffness matrix of the jamming based flexure mechanism can be determined by considering the stiffness in compression as well as bending [1], [2]. Here,

we consider the stiffness matrix in 2D as this includes the main directions in which jamming provides tunability.

$$\begin{bmatrix} F_x \\ F_y \\ M_z \end{bmatrix} = \begin{bmatrix} \frac{24EI}{L^3} & 0 & 0 \\ 0 & \frac{2Enbh}{L} & 0 \\ \frac{-12EI}{L^2} & 0 & \frac{EbnhD^2}{2L} \end{bmatrix} \times \begin{bmatrix} \delta_x \\ \delta_y \\ \theta \end{bmatrix} \tag{4}$$

When a sufficiently large force is applied (F_{yield} in Fig. 1C), the frictional force between the layers is exceeded and the layers slide (upper blue curve in Fig. 1C). This yield force is given by [16]

$$F_{yield} = \frac{8nbh\mu P}{3} \tag{5}$$

where nbh is the total surface area of each jamming element, P is the applied pressure, and μ is the coefficient of friction. This expression assumes that the deformation is small, such that the axial tension and compression induced in the jamming elements do not affect the shear force.

Equation 5 shows that the point of yield can be tuned on-the-fly by changing the vacuum pressure, introducing a tunable force threshold for yielding. This is significant since the range of motion of a traditional flexure is limited by the yield stress of the material, as plastic deformation must be avoided. With a jamming-based flexure, yield and plastic deformation occur on a structural level. Catastrophic failure is not an issue because the individual thin layers can experience proportionately higher deformation (curvature) before failure. This tunable yield point provides a controllable overload prevention feature that can prevent high forces in collisions. There is an added ability to reset after failure (yield), simply by unjamming and rejamming the structure.

At loads higher than F_{yield}, the layers slip with respect to each other, the stiffness of the structure is lower and energy is dissipated due to frictional sliding (blue shaded "damping" area in Fig. 1C). This enables damping which can be modulated with the applied vacuum pressure. Previous studies of the dynamic response of jamming structures have produced a lumped parameter model (Fig. 1D) which can be used to predict damping behavior [17]. When there is no vacuum applied, the coulomb friction damper is effectively inactive, the low stiffness spring (k_{low}) dominates and the system will thus have a lower natural frequency ($\omega_n = \sqrt{k/m}$). However, when a vacuum is applied, the damper locks, so the high stiffness spring (k_{high}) sets the dominant stiffness and the natural frequency of the jammed sample is much higher. When the applied force exceeds F_{yield}, the damper begins to slip and the incremental stiffness reverts to low stiffness spring (k_{low}). See [17] for further details.

B. Experimental Validation

Experimental validation of the foregoing models used the setup seen in Fig. 2A. Paper with a thickness of 0.1 mm and a Young's modulus of 5 GPa (HP Printer Paper Multipurpose 20, HP Inc., Palo Alto, CA, USA) was cut into 27.5 mm wide strips. Two stacks of these strips, each with 50 layers, were clamped 50 mm apart on the fixed support after being
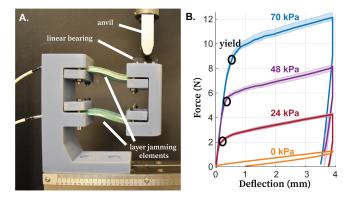
Fig. 2. Experimental characterization of a jamming-based parallel flexure mechanism. **A.** Experimental Setup. **B.** Force-displacement results. Lines represent means at each deflection and the shaded bars are the standard error across trials and samples.

encased in a TPE envelope (Stretchlon 200, FibreGlast DevelopmentsCorp., Brookville, OH, USA). The other ends of the structures were clamped to the free-end rigid component, leaving 45 mm long jamming elements. Force-displacement curves were obtained under varying vacuum levels using a materials testing device (Instron 5566, Illinois Tool Works, Norwood, MA, USA). The flexure structure was loaded from the top of its free end, with a linear bearing in the lateral direction under the driving anvil to prevent external axial loads. A pressure regulator (EW-07061-30, Cole-Parmer, Vernon Hills, IL, USA) controlled the vacuum level. Measurements were taken for no vacuum applied, 24 kPa, 48 kPa and 70 kPa, for two different jamming-based flexure specimens and for three trials for each vacuum condition.

The results are presented in Fig. 2B. In the no vacuum case (lower orange curve) a low stiffness of $k_{\delta_x F_x} = 0.33 N/mm$ is observed with minimal hysteresis, caused by the small amount of friction between the layers. This shows the slight disadvantage of jamming-based flexures over traditional flexures, since there will be a minor dead-zone. When vacuum is applied (upper three curves) a much higher initial stiffness of $k_{\delta_x F_x} = 20.2 N/mm$ is observed. This initial linear behavior is equal for the different vacuum conditions, and there is no friction at the jammed state before yield as the layers do not slip with respect to each other. The yield force at which the structure starts to exhibit low stiffness and dissipate energy is directly proportional to the applied pressure.

The experimental results confirm the model above with good repeatability. The difference between the jammed and unjammed stiffnesses show that the compliance of the flexures can be tuned over a wide range (an average of 63x), giving the opportunity to transition between degree of freedom and degree of constraint. The point of yield scales with the applied vacuum pressure to allow the flexure to act as a tunable, resettable, mechanical overload preventer. As seen in Fig. 2B, the stiffness is much lower after yield, resulting in a controllable maximum force. In addition, the hysteresis loop (area under the curve) is proportional to pressure, which enables variable damping. This permits tuning damping behavior and impact response, as demonstrated below.

III. JAMMING-BASED TUNABLE IMPEDANCE ROBOT WRIST

Jamming-based flexures are particularly promising for modulating passive impedance during contact tasks. Compliance (i.e. low stiffness) can minimize unwanted forces generated by positioning errors and avoid high impact forces during tasks such as contour tracking, assembly operations, and human-robot interaction [18]–[21]. On the other hand, high stiffness can enable accurate and fast motion control. The ability to vary stiffness in response to changing task requirements can thus simplify robot control and enhance performance in a wide range of tasks.

A. Wrist design

These advantages for manipulation tasks can be embodied in a wrist for mounting between a robot arm and an end effector. Fig. 3 shows a 2-DOF robot wrist with tunable stiffness and damping in orthogonal directions (red arrows), based on two jamming-based parallel flexure mechanisms in series. The upper blue component is the rigid end effector mounting and the bottom one is the robot arm mounting. The central blue component provides a series connection between the two parallel flexure structures which are each clamped to the mountings.
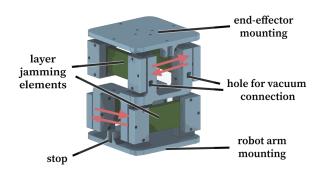

Fig. 3. A tunable impedance jamming-based robot wrist, with two directions of motion (red arrows) where each can transition between a DOF and a DOC.

Each parallel flexure mechanism has two jamming structures. Four stacks of paper , each stack composed of fifty layers (thickness of 0.1 mm, width of 2 cm and a Young's modulus of 5 GPa), are heat sealed inside an air-tight TPE envelope with a tube connecting to the vacuum pressure regulator. Each envelope also contains a layer of porous paper (Breather and Bleeder Cloth, FibreGlast DevelopmentsCorp., Brookville, OH, USA) to ensure the vacuum reaches the entire jamming element. The jamming elements have a bending length of 54 mm. The wrist also has two safety stops, limiting the range of motion in each direction of motion. The mass of the wrist is 265 g.

B. Experimental Methods

This tunable impedance wrist is used in two experiments to evaluate its capabilities in static and dynamic manipulation.

1) Hybrid Position/Force Control: Hybrid position/force control provides a means for decomposing task control into axes where either position or force should be controlled [22]. The tunable wrist provides a natural means for implementing this approach: compliant or stiff behavior can be programmed in each axis as required for the specific task.

To evaluate this capability, we use the wrist in a tracing/wiping task, such as washing a window or erasing a whiteboard. To perform this task, the robot moves its end effector (holding a sponge or eraser) over the surface while maintaining contact. Here the robot impedance in the direction perpendicular to the surface (z axis) should be compliant so that position errors do not generate large forces; in the directions parallel to the surface (x and y directions) the robot impedance should be stiff to maintain good position control despite varying frictional forces.

The jamming-based tunable wrist permits direct variation of end effector impedance in orthogonal axes, as required for this task. To validate this hypothesis, a simple end effector is attached to the robot wrist and a whiteboard eraser is attached (Fig. 5). A 6-axis force/torque sensor (HEX-58-RE-400N, OptoForce Ltd., Budapest, Hungary) is fixed to the bench and a whiteboard is mounted to the sensor. The position of the end effector and the robot mounting plate of the wrist is measured using an optical tracker (MicronTracker MTC 3.6, Claron Technology, Inc., Toronto, Canada).

The robot arm mounting is attached to a linear ball slide along the side of the whiteboard to provide repeatable motion. To simulate the effects of robot trajectory errors with respect to the environment, a misalignment between the robot path and the traced surface is introduced by raising one end of the linear ball slide to create an incline (Fig. 5). This misalignment causes the hand to be driven slightly into the

whiteboard, rather than only along its surface, so the contact forces (in the z direction) will reach large values if the end effector is stiff. Having an entirely compliant wrist would lower the contact forces, but this is not viable for this task as well-controlled positioning is desired in the direction of motion (x direction). Using this setup the robot wrist was
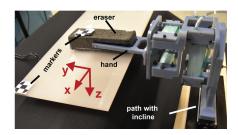

Fig. 5. Experimental setup for tracing task with jamming-based tunable impedance wrist. The eraser is moved back and forth along the x axis while applying a force in the z direction.

moved back and forth along the linear ball slide while force and position data was simultaneously collected (Fig. 4). The experiment was repeated for four conditions, capturing all the combinations of wrist impedance settings. In Condition I, the wrist is stiff in both axes so the end effector follows the input path with small x position error. This configuration, however, leads to higher z contact forces due to the incline misalignment between input trajectory and the whiteboard surface. At the other extreme, the wrist is fully compliant (Condition IV) the z forces are reduced, but a significant x position error is introduced.

In Condition III, the compliance along the x direction allows the frictional force between the whiteboard and the eraser to produce large x position errors. In addition, the
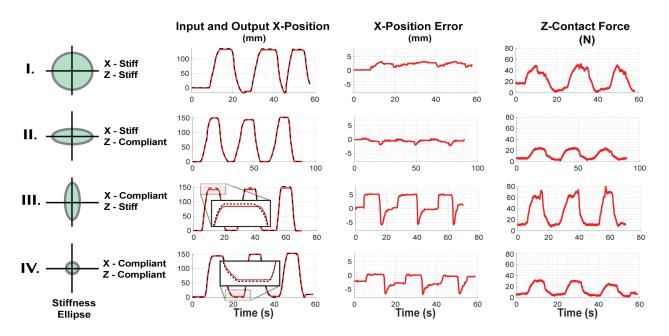

Fig. 4. Position and force data from the tracing task using the jamming-based flexure wrist. The experiment is conducted in four different conditions: **I.** Both axes stiffened; **II.** Only X-axis stiffened; **III.** Only Z-axis stiffened and **IV.** Both axes compliant. The dashed black line is the position input from the robot arm.

wrist is stiff along the z axis so large forces are generated by the misalignment. In Condition II, the wrist is stiff in the direction of desired precision (x) but compliant in the direction in which uncertainties are introduced (z). This provides the ideal arrangement: small position errors and low contact forces.

2) Impact Response: The proposed wrist design can also control the impact response of a robot. First, the jamming-based wrist introduces an intrinsic safety mechanism in desired directions, due to its yield point tunable with the applied pressure. This enables the setting of a force threshold which is introduced only when desired, in specified directions of motion. This mode of failure is also fully resettable, simply by unjamming (removing the vacuum) and rejamming (reapplying the vacuum) to the flexures.

The wrist can also provide a tunable damping response. The jamming based flexures in the wrist act as coulomb friction dampers, and the amount of energy dissipated (area under the curves in Fig. 2B) can be tuned by changing the vacuum pressure. When the structures are unjammed there is effectively no energy dissipation, so there will be no damping. When the applied pressure is too high, the yield force will be much larger than desired and the structure will respond elastically without dissipating energy. For pressures in the middle, the amount of energy dissipated can be tuned to match the desired response.

To experimentally characterize the impact response of the jamming-based tunable impedance wrist, we applied a impulse force to the wrist and recorded its response under varying vacuum levels. The wrist's robot arm mounting plate was mounted on the optical force sensor then a pendulum consisting of a 75 g mass was released from a fixed height (Fig. 6). Three trials were conducted at each vacuum pressures of 0, 15, and 60 kPa.

Force vs. time response curves (Fig. 6) show that for highest vacuum pressure (60 kPa), the peak impact force of 31.6 N is significantly greater than in the other conditions. This is because the high yield force means the structure does not start dissipating energy until the force reaches this high yield force level and the layers begin to slide against each other. In addition, high-frequency oscillations persist for many cycles due to the high stiffness (k_{hi} in Fig. 1D) combined with the high yield force.

In contrast, with no vacuum pressure (0 kPa), the 13.3 N peak force is much smaller, but oscillation persist due to the lack of frictional damping. The vibration frequency is much lower (at 25 Hz) due to the lower stiffness (k_{low} in Fig. 1D). At the intermediate pressure of 15 kPa, however, the peak force is reduced to 19.6 N, the settling time is much shorter, and the oscillation amplitude is the smallest of the pressure levels. This demonstrates the ability of jamming-based flexure mechanisms to modulate impact response.

IV. DISCUSSION

This study introduces layer jamming based flexure mechanisms, which have the advantages of traditional flexure mechanisms, combined with the ability to change between degrees
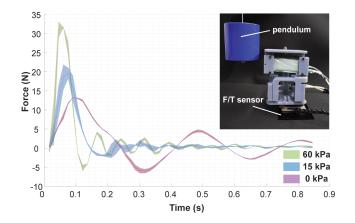

Fig. 6. Impact response of the tunable impedance wrist. A pendulum was released from a constant height, impacting the end-effector mounting plate. The vacuum pressure supplied to the jamming structures was set to 0, 15, and 60 kPa. The lines show the mean from three trials in each condition and the shaded areas are the standard deviations.

of freedom and degrees of constraint, the option to limit peak forces during impacts by acting as a mechanical overload preventer, and the ability to tune damping to control impacts. Moreover, these advantages are inherent characteristics of the flexure structures, minimizing construction complexity and simplifying execution of contact tasks.

The study also proposes a jamming-based tunable impedance robot wrist which enables hybrid position/force control utilizing 'mechanical intelligence,' i.e. passive mechanics tuned to achieve the desired behavior. Hybrid position/force control is traditionally implemented using active sensing and control [7], [22]. This novel wrist design, by introducing directionally-controllable compliance that activates degrees of freedom as needed, reduces the need for active control while guaranteeing effective mechanical interactions.

The jamming-based flexure prototypes evaluated in this study demonstrated a large variation in controllable stiffness (63x), which is more than adequate for the proposed robotic applications envisioned here. This range, however, was significantly smaller than predicted by the models (2500x), although these models showed good agreement with prior experimental tests [16], [17]. A major difference is the boundary conditions required by flexures, i.e. fully-constrained double-cantilever ends, as opposed to simple-cantilevers with one free end or three-point bending with both free ends, as used in prior studies. The fully constrained ends cause a larger unjammed stiffness than the model's prediction (twice as large) since the model assumes the layers are completely decoupled in the unjammed state. When jammed, on the other hand, the minute differences in lengths of layers between the two clamps, result in discontinuous surface contact due to the differing arc lengths. This results in a lower pre-slip stiffness (18 times smaller) than the model's prediction. We are working to develop high-precision fabrication and assembly techniques to minimize this effect and increase the stiffness variation range. We note that the 63-fold change in stiffness attained here is

larger than the range obtained with most variable stiffness actuators and transmissions [10]. A number of flexures with tunable responses have been previously developed. These include piezoelectric based flexures [23] and shape memory polymer flexures [24], [25]. The jamming-based flexures reported here introduce a new option with greater stiffness range, more versatility, and a simple and low-cost design which does not require electromechanical components or high temperatures. Similarly, robotic wrists with tunable impedance (e.g. [18], [26]) have required more complex construction and control than this approach. The jamming-based flexure approach introduced here can be extended in a number of ways. While damping and yield force can be modulated by vacuum pressure, stiffness change is binary in layer jamming structures with all layers enclosed in a single envelope. This can be extended to allow for a variety of stiffness values by introducing multiple jamming elements within the flexure, each with a different number of layers. By selectively applying vacuum to combinations of jamming elements the stiffness can be varied. This concept could be useful for robotic systems in which different stiffnesses are required, such as haptic interfaces. The 2-DOF wrist concept can be extended to additional degrees of freedom by utilizing the wide abundance of compound flexure mechanisms in the mechanical design literature. The approach presented here leverages flexure systems' ability to adapt to complex degrees of freedom, with tunable static and dynamic responses. This can enable more complex motions and task interactions.

V. CONCLUSIONS

This work has introduced layer jamming based flexure mechanisms, which seamlessly combine the advantages of flexure systems with tunable stiffness and damping systems. These mechanisms have the ability to switch between degrees of freedom and degrees of constraint, to act as a 'mechanical circuit breaker' allowing for a resettable overload prevention safety mechanism, and to have a tunable impact response through variable damping. These versatile functions have been demonstrated experimentally, and analytical models are provided to enable designers to predict the effect of different design parameters on the behavior of these structures. A tunable impedance jamming-based wrist which utilizes the jamming-based flexure mechanisms is also presented, verifying that these flexures structures are a design platform which can be used to create complex robotic systems with hybrid position/force control through tunable compliance along different directions of motion.

ACKNOWLEDGMENTS

REFERENCES

[1] S. Smith, *Flexures:elements of elastic mechanisms*. CRCPress, 2014.
[2] L. L. Howell, *Compliant mechanisms*. John Wiley & Sons, 2001.
[3] Y. Li and Q. Xu, "Design and analysis of a totally decoupled flexure-based xy parallel micromanipulator," *IEEE Transactions on Robotics*, vol. 25, no. 3, pp. 645–657, 2009.

[4] G. Chung, K. Choi, and J. Kyung, "Development of precision robot manipulator using flexure hinge mechanism," in *2006 IEEE Conference on Robotics, Automation and Mechatronics*, June 2006, pp. 1–6.
[5] M. Goldfarb and N. Celanovic, "A flexure-based gripper for small-scale manipulation," *Robotica*, vol. 17, no. 2, pp. 181–187, 1999.
[6] D. Y. Choi and C. N. Riviere, "Flexure-based manipulator for active handheld microsurgical instrument," in *2005 IEEE Engineering in Medicine and Biology 27th Annual Conference*. IEEE, 2006, pp. 2325–2328.
[7] N. Hogan, "Impedance control - an approach to manipulation," *ASME, Transactions, Journal of Dynamic Systems, Measurement, and Control*, vol. 107, pp. 1–24, 1985.
[8] R. J. Anderson and M. W. Spong, "Hybrid impedance control of robotic manipulators," *IEEE Journal on Robotics and Automation*, vol. 4, no. 5, pp. 549–556, 1988.
[9] K. F. Laurin-Kovitz, J. E. Colgate, and S. D. Carnes, "Design of components for programmable passive impedance," in *Proceedings. 1991 IEEE International Conference on Robotics and Automation*. IEEE, 1991, pp. 1476–1481.
[10] S. Wolf et al., "Variable Stiffness Actuators: Review on Design and Components," *IEEE/ASME Transactions on Mechatronics*, vol. 21, no. 5, pp. 2418–2430, 2016.
[11] R. v. Ham, T. Sugar, B. Vanderborght, K. Hollander, and D. Lefeber, "Compliant actuator designs," *IEEE Robotics & Automation Magazine*, vol. 3, no. 16, pp. 81–94, 2009.
[12] M. Manti, V. Cacucciolo, and M. Cianchetti, "Stiffening in Soft Robotics," *IEEE Robotics & Automation Magazine*, pp. 93–106, 2016.
[13] L. Blanc, A. Delchambre, and P. Lambert, "Flexible Medical Devices: Review of Controllable Stiffness Solutions," *Actuators*, vol. 6, no. 3, p. 23, 2017.
[14] Y.-J. Kim, S. Cheng, and S. Kim, "A Novel Layer Jamming Mechanism With Tunable Stiffness Capability for Minimally Invasive Surgery," *IEEE Transactions on Robotics*, vol. 29, no. 4, pp. 1–12, 2015.
[15] J. L. C. Santiago, I. S. Godage, P. Gonthina, and I. D. Walker, "Soft Robots and Kangaroo Tails: Modulating Compliance in Continuum Structures Through Mechanical Layer Jamming," *Soft Robotics*, vol. 3, no. 2, pp. 54–63, 2016.
[16] Y. S. Narang, J. J. Vlassak, and R. D. Howe, "Mechanically Versatile Soft Machines through Laminar Jamming," *Advanced Functional Materials*, vol. 28, no. 17, p. 1707136, 2018.
[17] Y. S. Narang, A. Degirmenci, J. J. Vlassak, and R. D. Howe, "Transforming the dynamic response of robotic structures and systems through laminar jamming," *IEEE Robotics and Automation Letters*, vol. 3, no. 2, pp. 688–695, 2018.
[18] R. P. Xu, Yangsheng; Paul, "A Robot Compliant Wrist System for Automated Assembly," *IEEE International Conference on Robotics and Automation*, 1990.
[19] Y. She, H.-J. Su, C. Lai, and D. Meng, "Design and prototype of a tunable stiffness arm for safe human-robot interaction," in *ASME 2016 International Design Engineering Technical Conferences and Computers and Information in Engineering Conference*. American Society of Mechanical Engineers, 2016, pp. V05BT07A063–V05BT07A063.
[20] S. Wolf and G. Hirzinger, "A new variable stiffness design: Matching requirements of the next robot generation," in *2008 IEEE International Conference on Robotics and Automation*. IEEE, 2008, pp. 1741–1746.
[21] T. Morita and S. Sugano, "Development of one-dof robot arm equipped with mechanical impedance adjuster," in *Proceedings 1995 IEEE/RSJ International Conference on Intelligent Robots and Systems*, vol. 1. IEEE, 1995, pp. 407–412.
[22] M. H. Raibert and J. J. Craig, "Hybrid position/force control of manipulators," *Journal of Dynamic Systems, Measurement, and Control*, vol. 103, no. 2, pp. 126–133, 1981.
[23] X. Chen, Zhong; Chen, Guisheng; Zhang, "Damped leaf flexure hinge," *Review of Scientific Instruments*, vol. 86, p. 055002, 2015.
[24] L. Hines, V. Arabagi, and M. Sitti, "Shape Memory Polymer-Based Flexure Stiffness Control in a Miniature Flapping-Wing Robot," *IEEE Transactions on Robotics*, vol. 28, no. 4, pp. 987–990, 2012.
[25] Y. Bellouard and R. Clavel, "Shape memory alloy flexures," *Materials Science and Engineering: A*, vol. 378, no. 1-2, pp. 210–215, 2004.
[26] M. Cutkosky and P. Wright, "Active control of a compliant wrist in manufacturing tasks," *Journal of Engineering for Industry*, vol. 108, no. 1, pp. 36–43, 1986.